

# Graph Neural Networks with Convolutional ARMA Filters

Filippo Maria Bianchi<sup>1</sup> Daniele Grattarola<sup>2</sup> Cesare Alippi<sup>2,3</sup> Lorenzo Livi<sup>4,5</sup>

## Abstract

Recent graph neural networks implement convolutional layers based on polynomial filters operating in the spectral domain. In this paper, we propose a novel graph convolutional layer based on auto-regressive moving average (ARMA) filters that, compared to the polynomial ones, provide a more flexible response thanks to a rich transfer function that accounts for the concept of state. We implement the ARMA filter with a recursive and distributed formulation, obtaining a convolutional layer that is efficient to train, is localized in the node space and can be applied to graphs with different topologies. In order to learn more abstract and compressed representations in deeper layers of the network, we alternate pooling operations based on node decimation with convolutions on coarsened versions of the original graph. We consider three major graph inference problems: semi-supervised node classification, graph signal classification, and graph classification. Results show that the proposed graph neural network with ARMA filters outperforms those based on polynomial filters and sets the new state of the art in several tasks.

## 1. Introduction

Several deep learning architectures have been proposed for data represented as graphs. The well-established Convolutional Neural Networks (CNNs) (Krizhevsky et al., 2012) convolve an input tensor with a small trainable kernel of the same rank, applied to fixed-size volumes. The inductive bias entailed by the convolutional kernel yields locality and translation invariance in space, which works well for regu-

lar grids, but prevents to capture the variability of a graph structure. Therefore, to apply CNNs on graphs, different approaches have been proposed to modify the convolution operator (Atwood & Towsley, 2016; Monti et al., 2017; Fey et al., 2018) or to locally approximate a graph with a regular structure before applying the traditional spatial convolution (Niepert et al., 2016; Zhang et al., 2018).

Graph Neural Networks (GNNs) constitute a class of recently developed tools lying at the intersection between deep learning and methods for structured data, which perform inference on discrete objects (assigned to nodes) by accounting for arbitrary relationships (edges) among them (Battaglia et al., 2018). A GNN combines node features within local neighborhoods on the graph to learn graph embeddings (Perozzi et al., 2014; Duvenaud et al., 2015; Yang et al., 2016; Hamilton et al., 2017; Bacciu et al., 2018), or to directly perform inference tasks by mapping the node features into categorical labels or real values (Scarselli et al., 2009; Micheli, 2009).

Of particular interest for this work are those GNNs that implement a convolution operation in the spectral domain with a nonlinear trainable filter, which maps the node features in a new space (Bruna et al., 2013; Henaff et al., 2015). To avoid computing the expensive spectral decomposition and projection in the frequency domain, state-of-the-art GNNs approximate graph filters with finite order polynomials (Defferrard et al., 2016; Kipf & Welling, 2016a,b). Polynomial filters have a finite impulse response (FIR) and realize a weighted moving average filtering of graph signals on local node neighbourhoods (Tremblay et al., 2018), thus allowing for fast distributed implementations based on Chebyshev polynomials and Lanczos iterations (Susnjara et al., 2015; Defferrard et al., 2016; Liao et al., 2019). Despite their attractive computational efficiency, FIR filters are sensitive to changes in the graph signal (an instance of the node features) or in the underlying graph structure (Isufi et al., 2016). Moreover, polynomial filters are very smooth and cannot model sharp changes in the frequency response (Tremblay et al., 2018). A more versatile class of filters is the family of Auto-Regressive Moving Average filters (ARMA) that allow for a more accurate filter design and, in several cases, give exact rather than approximate solutions in modeling the desired response (Narang et al., 2013).

<sup>1</sup>Machine Learning Group, UiT the Arctic University of Tromsø, Norway <sup>2</sup>Faculty of Informatics, Università della Svizzera Italiana, Switzerland <sup>3</sup>Dept. of Electronics, Information, and Bioengineering, Politecnico di Milano, Italy <sup>4</sup>Dept. of Computer Science and Mathematics, University of Manitoba, Canada <sup>5</sup>Dept. of Computer Science, University of Exeter, United Kingdom. Correspondence to: Filippo Maria Bianchi <filippo.m.bianchi@uit.no>.

**Contribution** In this paper, we address the limitations of existing graph convolutional layers in modeling a desired filter response and propose a GNN based on a novel ARMA layer. The ARMA layer implements a non-linear and trainable ARMA graph filter that generalizes existing graph convolutional layers based on polynomial filters, and provides the GNN with enhanced modeling capability thanks to a flexible design of the filter transfer function. Contrarily to polynomial filters, ARMA filters are not localized in the node space, making their implementation inefficient within a GNN. To address this scalability issue, the proposed ARMA layer relies on a recursive formulation, which leads to a fast and distributed implementation that exploits efficient sparse operations on tensors. The resulting filters are not learned in the Fourier space induced by a given Laplacian, but are local in the node space and independent from the underlying graph structure. This allows our GNN to process graphs with different topologies.

When training deeper networks we adopt a node pooling procedure based on node decimation, inspired by the multi-resolution framework adopted in graph signal processing (Shuman et al., 2016). This allows us to build GNNs that yield more abstract representations in deeper layers of the network. Given an input graph, node decimation drops approximately half of its nodes and a coarsened version of the graph on the remaining ones is obtained through graph reduction. Pooling of different strides is implemented in the GNN by means of multiplications with pre-computed matrices.

To assess the performance of our GNN, we apply it to semi-supervised node classification, graph signal classification, and graph classification. Results show that the proposed GNN with ARMA filters outperforms GNNs based on polynomial filters, setting the new state of the art in several tasks.

## 2. Spectral filtering in GNNs

We assume a graph with  $M$  nodes to be characterized by a symmetric adjacency matrix  $\mathbf{A} \in \mathbb{R}^{M \times M}$  and we refer to *graph signal*  $\mathbf{X} \in \mathbb{R}^{M \times F}$  as the instance of all features (vectors in  $\mathbb{R}^F$ ) associated with the graph nodes. Let  $\mathbf{L} = \mathbf{I}_M - \mathbf{D}^{-1/2} \mathbf{A} \mathbf{D}^{-1/2}$  be the symmetrically normalized Laplacian ( $\mathbf{D}$  is the degree matrix), with spectral decomposition  $\mathbf{L} = \sum_{m=1}^M \lambda_m \mathbf{u}_m \mathbf{u}_m^T$ . A graph filter is a linear operator that modifies the components of  $\mathbf{X}$  on the eigenvectors basis of  $\mathbf{L}$ , according to a transfer function  $h$  acting on each eigenvalue  $\lambda$ . The filtered graph signal reads

$$\begin{aligned} \bar{\mathbf{X}} &= \sum_{m=1}^M h(\lambda_m) \mathbf{u}_m \mathbf{u}_m^T \mathbf{x}_m, \\ &= \mathbf{U} \text{diag}[h(\lambda_1), \dots, h(\lambda_M)] \mathbf{U}^T \mathbf{X} \end{aligned} \quad (1)$$

This formulation inspired the seminal work of Bruna et al. (2013) that implemented spectral graph convolutions in a neural network. Their GNN learns end-to-end the parameters of each filter implemented as  $h = \mathbf{B}\mathbf{c}$ , where  $\mathbf{B} \in \mathbb{R}^{M \times K}$  is a cubic B-spline basis and  $\mathbf{c} \in \mathbb{R}^K$  is a vector of control parameters. Those filters are not localized, since the full projection of the eigenvectors yields paths of infinite length and the filter accounts for interactions of each node with the whole graph, rather than those limited to the node neighborhood. Since this contrasts with the local design of classic convolutional filters, Henaff et al. (2015) introduced a parametrization of the spectral filters with smooth coefficients to achieve spatial localization. However, the main issue with such spectral filtering (1) is the computational complexity: not only the eigendecomposition of  $\mathbf{L}$  is expensive, but a double product with  $\mathbf{U}$  must be computed whenever the filter is applied. Notably,  $\mathbf{U}$  in (1) is full even when  $\mathbf{L}$  is sparse. Finally, since spectral filters depend on their specific Laplacian spectrum, they cannot be applied to graphs with different structure.

### 2.1. Chebyshev polynomial filters

The desired transfer function  $h(\lambda)$  can be approximated by a polynomial of order  $K$ ,

$$h_{\text{POLY}}(\lambda) = \sum_{k=0}^K w_k \lambda^k, \quad (2)$$

which performs a weighted moving average of the graph signal (Tremblay et al., 2018). Polynomial filters are localized in space, since the output at each node in the filtered signal is a linear combination of the nodes in its  $K$ -hop neighbourhood. A localized filter overcomes an important limitation of spectral formulations relying on a fixed Laplacian spectrum, making it suitable also for inference tasks on graphs with different structures (Zhang et al., 2018).

Compared to conventional polynomials, Chebyshev polynomials attenuate unwanted oscillations around the cut-off frequencies (Shuman et al., 2011). Chebyshev polynomials are exploited to implement fast localized filters in a GNN, avoiding to eigen-decompose the Laplacian by approximating the filter convolution with Chebyshev expansion  $T_k(x) = 2xT_{k-1}(x) - T_{k-2}(x)$  (Defferrard et al., 2016). It follows that the convolutional layers perform the filtering operation

$$\bar{\mathbf{X}} = \sigma \left( \sum_{k=0}^{K-1} T_k(\tilde{\mathbf{L}}) \mathbf{X} \mathbf{W}_k \right), \quad (3)$$

where  $\tilde{\mathbf{L}} = 2\mathbf{L}/\lambda_{\max} - \mathbf{I}_M$ ,  $\sigma$  is a non-linear activation (e.g., ReLU), and  $\mathbf{W}_k \in \mathbb{R}^{F_{\text{in}} \times F_{\text{out}}}$  are the  $k$  trainable weight matrices that map the node's features from an input space  $\mathbb{R}^{F_{\text{in}}}$  to a new space  $\mathbb{R}^{F_{\text{out}}}$ .

## 2.2. First-order polynomial filters

A first-order polynomial filter is adopted by Kipf & Welling (2016a) to solve the task of semi-supervised node classification. They propose a GNN called Graph Convolutional Network (GCN), where the convolutional layer is a simplified version of Chebyshev filters

$$\bar{\mathbf{X}} = \sigma(\hat{\mathbf{A}}\mathbf{X}\mathbf{W}). \quad (4)$$

Their formulation is obtained from (3) by considering only  $K = 1$  and setting  $\mathbf{W} = \mathbf{W}_0 = -\mathbf{W}_1$ . Additionally,  $\tilde{\mathbf{L}}$  is replaced by  $\hat{\mathbf{A}} = \tilde{\mathbf{D}}^{-1/2}\tilde{\mathbf{A}}\tilde{\mathbf{D}}^{-1/2}$ , with  $\tilde{\mathbf{A}} = \mathbf{A} + \mathbf{I}_M$ . In respect to  $\tilde{\mathbf{L}}$ ,  $\hat{\mathbf{A}}$  contains self-loops that compensate for the removal of the term of order 0 in the polynomial filter, ensuring that a node is part of its 1st order neighbourhood, and that its features are preserved after the convolution. The convolution with higher-order neighbourhoods can be obtained by stacking multiple layers. However, since each layer (4) performs a Laplacian smoothing, after few convolutions the node features becomes too smoothed over the graph (Li et al., 2018)

## 3. The ARMA graph convolutional layer

The polynomial filters discussed in the previous section are sensitive to changes in the graph signal or in the underlying graph structure, and their smoothness prevents to model filter responses with sharp changes. Moreover, they have poor interpolation and extrapolation capability around the known graph frequencies (Isufi et al., 2016). On the other hand, an ARMA filter approximates better the optimal  $h$  thanks to a rational design that allows to model a larger variety of filter shapes (Tremblay et al., 2018). The filter response of an ARMA( $P, Q$ ) reads

$$h_{\text{ARMA}}(\lambda) = \frac{\sum_{q=0}^Q b_q \lambda^q}{1 + \sum_{p=1}^P a_p \lambda^p}, \quad (5)$$

which in the node domain translates to the filtering relation

$$\bar{\mathbf{X}} = \frac{\left(\sum_{q=0}^Q b_q \mathbf{L}^q\right) \mathbf{X}}{1 + \sum_{p=1}^P a_p \mathbf{L}^p}. \quad (6)$$

The Laplacian appearing in the denominator implies a matrix inversion and multiplication between dense matrices, which is inefficient to implement in a GNN. To circumvent this issue, CayleyNets (Levie et al., 2019b) approximate the inverse with a fixed number of Jacobi iterations, by using a special formulation to avoid numerical instability. A more straightforward approach is to completely avoid the inverse computation and approximate the effect of an ARMA(1,0) filter with a first-order recursion

$$\bar{\mathbf{X}}^{(t+1)} = a\mathbf{M}\bar{\mathbf{X}}^{(t)} + b\mathbf{X}. \quad (7)$$

The eigenvalues of  $\mathbf{M} = \frac{1}{2}(\lambda_{\max} - \lambda_{\min})\mathbf{I} - \mathbf{L}$  are related to those of the Laplacian  $\mathbf{L}$  as follows:  $\mu_n = (\lambda_{\max} - \lambda_{\min})/2 - \lambda_n$ . The frequency response of the approximated ARMA(1,0) filter is

$$h_{\text{ARMA}}(\mu) = \frac{r}{\mu - p} \quad \text{with } r = -\frac{b}{a} \quad \text{and } p = \frac{1}{a}. \quad (8)$$

The recursive application of Eq. (7) is adopted in graph signal processing to apply a low-pass filter on a graph signal (Loukas et al., 2015), but (7) is also equivalent to the recurrent update used in Label Propagation (Zhou et al., 2004) and Personalized Page Rank (Page et al., 1999) to propagate information on a graph with a restart probability.

The effect of an ARMA( $K, K-1$ ) filter, as in (5), is simply obtained by summing the outputs of  $K$  ARMA(1,0) filters

$$\bar{\mathbf{X}} = \sum_{k=1}^K \bar{\mathbf{X}}_k = \sum_{k=1}^K \sum_{n=1}^M \frac{r_k}{\mu_m + p_k} \mathbf{u}_m \mathbf{u}_m^T \mathbf{x}_m. \quad (9)$$

### 3.1. Recursive and distributed implementation of the ARMA layer

Here we propose a recursive implementation of the ARMA filter based on neural networks (see Fig. 1). Eq. (7) must be applied many times before converging to a steady state. Instead, to obtain a more efficient implementation, we apply the recursive update only a few times and compensate by adding a non-linearity and trainable parameters.

We implement the recursive update in (7) with a *Graph Convolutional Skip* (GCS) layer, defined as

$$\bar{\mathbf{X}}^{(t+1)} = \sigma\left(\tilde{\mathbf{L}}\bar{\mathbf{X}}^{(t)}\mathbf{W}^{(t)} + \mathbf{X}\mathbf{V}^{(t)}\right), \quad (10)$$

where  $\mathbf{W}^{(t)} \in \mathbb{R}^{F_{\text{out}}^t \times F_{\text{out}}^{t+1}}$  and  $\mathbf{V}^{(t)} \in \mathbb{R}^{F_{\text{in}} \times F_{\text{out}}^{t+1}}$  are trainable parameters; we set  $\bar{\mathbf{X}}^{(0)} = \mathbf{X}$ . The modified Laplacian matrix  $\tilde{\mathbf{L}} = \mathbf{I} - \mathbf{L}$  is derived by setting  $\lambda_{\min} = 0$  and  $\lambda_{\max} = 2$  in  $\mathbf{M}$ . This is a reasonable simplification, since the spectrum of  $\mathbf{L}$  lies in  $[0, 2]$  and the trainable parameters in  $\mathbf{W}^{(t)}$  can compensate for the small offset introduced. Each GCS layer extracts local substructure information by aggregating node information in local neighbourhoods and, through the skip connection, by combining them with the original node features. The computational complexity of GCS layers is linear in the number of edges, and can be efficiently implemented as a sparse product of  $L$  and  $X$ .

We build  $K$  parallel stacks, each one with  $T$  GCS layers, and define the output of the ARMA convolutional layer as

$$\bar{\mathbf{X}} = \text{avgpool}\left(\sum_{k=1}^K \bar{\mathbf{X}}_k^{(T)}\right), \quad (11)$$

where  $\bar{\mathbf{X}}_k^{(T)}$  is the last output of the  $k$ -th stack. We apply dropout to the skip connection of each GCS layer not only

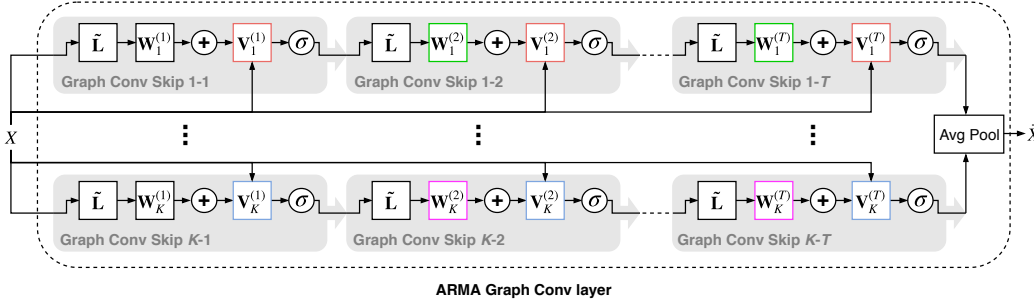


Figure 1. The ARMA convolutional layer. Same colour indicates shared weights.

for regularization, but also to encourage diversity in the filters learned in each one of the  $K$  parallel stacks. To provide a further regularization and reduce the number of parameters in the ARMA layer, the GCS layers in each stack may share the same parameters, except for  $\mathbf{W}_k^{(1)} \in \mathbb{R}^{F_{in} \times F_{out}}$  that performs a different mapping in the first layer of the stack. Namely,  $\mathbf{W}_k^{(i)} = \mathbf{W}_k^{(i+1)} = \mathbf{W}_k \in \mathbb{R}^{F_{out} \times F_{out}}, \forall i > 1$  and  $\mathbf{V}_k^{(i)} = \mathbf{V}_k^{(i+1)} = \mathbf{V}_k \in \mathbb{R}^{F_{in} \times F_{out}}, \forall i$ . Note that since each stack of GCS layers is independent from the others, it is possible to distribute the computation of an ARMA layer across multiple processing units.

### 3.2. Properties and relationship with other approaches

Contrarily to filters defined in the spectral domain (Bruna et al., 2013), ARMA filters do not explicitly depend on eigenvectors and eigenvalues, making them robust to perturbations in the underlying graph. For this reason, as formally proven for generic rational filters by Levie et al. (2019a), the proposed ARMA filters are stable and transferable, i.e., they can generalize to graph signals not seen during training and graphs with different topologies. Contrarily to polynomial filters, in the ARMA layer  $\mathbf{L}$  is not exponentiated and remains sparse; this implies faster computations since  $\mathbf{L}$  becomes quickly dense ( $\mathbf{L}^P$  describes a fully connected graph if  $P$  is the graph diameter, which is usually small in real-world networks). The ARMA layer can naturally deal with time-varying graph signals (Holme, 2015; Grattarola et al., 2018) by replacing the constant term  $\mathbf{X}$  in (10) with a time-dependent input  $\mathbf{X}^{(t)}$ . The GCS layer has a similar formulation to the graph convolutional layer in (4); however, thanks to the skip connection, it is possible to stack multiple layers without risking to over-smooth the node features (Li et al., 2018). The formulation of the ARMA layer with shared weights is similar to recurrent neural networks with residual connections (Wu et al., 2016). Finally, similarly to GNNs operating in the node domain (Scarselli et al., 2009; Gallicchio & Micheli, 2010), each GCS layer computes the filtered signal  $\bar{\mathbf{x}}_i^{(t+1)}$  at vertex  $i$  as a combination of signals  $\mathbf{x}_j^{(t)}$  in its 1-hop neighborhood,  $j \in \mathcal{N}(i)$ ; such a commutative aggregation solves the problem of undefined vertex ordering and varying neighborhood sizes.

## 4. Node Pooling

Node pooling is particularly important in tasks like graph (signal) classification, in order to associate a label to a graph. Contrarily to other neural networks, that operate exclusively on the input signal, GNNs require to coarsen the original graph to perform further convolutions as the graph signal is reduced through the network layers.

A recent approach (Ying et al., 2018) proposes to learn differentiable soft assignments to cluster the nodes at each layer. The original adjacency matrix acts as a prior when learning the soft assignment and sparsity is enforced with an entropy-based regularization. However, the application of this method to medium and large graphs is not feasible, as it introduces a number of additional trainable parameters quadratic in the number of nodes. Another approach followed in most GNNs consists of pre-computing coarsened versions of the graph using hierarchical clustering (Bruna et al., 2013; Defferrard et al., 2016; Monti et al., 2017; Fey et al., 2018). At each level  $l$ , two vertices  $x_i^{(l)}$  and  $x_j^{(l)}$  are clustered together in a new vertex  $x_z^{(l+1)}$ . Then, a standard pooling operation is applied to halve the size of the graph signal. To make the pooling output consistent with the cluster assignment, the graph signal is rearranged so that elements  $i$  and  $j$  end up in consecutive positions. This approach has several drawbacks. First, the connectivity of the original graph is not preserved in the coarsened graphs and the spectrum of their associated Laplacians is usually not contained in the spectrum of the original Laplacian. Second, the procedure to rearrange vertices is cumbersome to implement; moreover, it requires to add fake vertices so that the number of nodes can be halved each time, hence injecting noisy information in the graph signal. Finally, the clustering result depends on the initial order of the nodes, which hampers stability and reproducibility.

In this paper, we use a pooling procedure that builds on the multi-resolution framework adopted in graph signal processing (Shuman et al., 2016), which addresses the drawbacks of the aforementioned methods. A similar, yet preliminary approach was recently discussed by Simonovsky & Komodakis (2017). Here, we provide a more detailed formulation framed within the GNN framework of pooling based on node decimation and of graph reduction, which



generates a new coarsened graph where ensuing convolutions are applied. The experiments give a systematic comparison with respect to pooling based on graph clustering.

#### 4.1. Node decimation pooling and graph reduction

**Pooling with node decimation.** A simple way to decimate nodes  $\mathcal{V}$  of an arbitrary graph consists of partitioning them in two sets based on the largest eigenvector  $\mathbf{u}_{\max}$  of the Laplacian, and then drop one of the two sets of nodes. In particular, the pooling operation keeps only the nodes in the set  $\mathcal{V}^+$

$$\mathcal{V}^+ = \{n \in \mathcal{V} : \mathbf{u}_{\max}(n) \geq 0\}. \quad (12)$$

We note that keeping  $\mathcal{V}^+$  is equivalent to keeping  $\mathcal{V}^-$ , i.e., the nodes associated with a negative value in  $\mathbf{u}_{\max}$ . A partition of  $\mathcal{V}$  can also be obtained by clustering the values in  $\mathbf{u}_{\max}$  with  $k$ -means ( $k = 2$ ). Despite its simplicity, this procedure offers important advantages: i) approximately half of the nodes are removed each time, i.e.,  $|\mathcal{V}^+| \approx |\mathcal{V}^-|$ ; ii) the nodes in  $\mathcal{V}^+$  and  $\mathcal{V}^-$  are connected by edges with small weights; iii)  $\mathbf{u}_{\max}$  can be quickly computed with the power method. Furthermore, compared to the pooling based on graph clustering, this approach does not require to introduce fake nodes and to reorder nodes according to their cluster indices.

The pooling operation is implemented by multiplying a graph signal  $\mathbf{X}$  with a *decimation matrix*  $\mathbf{S}$ , which is obtained by keeping in the identity matrix  $\mathbf{I}_M$  only the rows corresponding to the vertices in  $\mathcal{V}^+$ ,

$$\mathbf{X}_{\text{pool}} = \mathbf{S}\mathbf{X} = [\mathbf{I}_M]_{\mathcal{V}^+, \mathcal{V}} \mathbf{X}. \quad (13)$$

**Graph reduction.** A simple approach to reduce the original Laplacian to a new Laplacian  $\mathbf{L}^{\text{new}}$  defined on the subset  $\mathcal{V}^+$  consists of computing

$$\mathbf{L}^{\text{new}} = ([\mathbf{L}]^2)_{\mathcal{V}^+, \mathcal{V}^+}, \quad (14)$$

which are the selected rows and columns of the 2-hop Laplacian (Narang & Ortega, 2010). Since the decimation operation ideally removes the first-closest neighbour of nodes  $\mathcal{V}^+$  (i.e., the nodes in  $\mathcal{V}^-$ ), it is intuitive that before being dropped the nodes should propagate their information in the first-order neighbourhood. While this graph reduction is very fast to compute, it does not always preserve connectivity, it introduces self-loops, and the spectra of  $\mathbf{L}$  and  $\mathbf{L}^{\text{new}}$  may not be interlaced (i.e., the spectrum of  $\mathbf{L}^{\text{new}}$  may not be contained in the spectrum of  $\mathbf{L}$ ).

The Kron reduction (Shuman et al., 2016) is a more advanced technique that defines the reduced Laplacian as

$$\mathbf{L}^{\text{new}} = \mathbf{L}_{\mathcal{V}^+, \mathcal{V}^+} - \mathbf{L}_{\mathcal{V}^+, \mathcal{V}^-} \mathbf{L}_{\mathcal{V}^-, \mathcal{V}^-}^{-1} \mathbf{L}_{\mathcal{V}^-, \mathcal{V}^+} \quad (15)$$

The resulting  $\mathbf{L}^{\text{new}}$  is a well-defined Laplacian where two nodes are connected only if there is a path between them in the original  $\mathbf{L}$ . Furthermore,  $\mathbf{L}^{\text{new}}$  does not introduce self-loops and guarantees spectral interlacing and resistance distance preservation (Shuman et al., 2016). The main drawback compared to (14) is the computation of the inverse, which can give memory issues in very large graphs.

**Graph Sparsification.** Due to the connectivity preservation property, after each Kron reduction  $\mathbf{L}^{\text{new}}$  becomes denser and its connectivity less localized. This implies more computation in the deeper layers, since the complexity of graph convolutions scales with the number of edges. A solution is to apply spectral sparsification (Batson et al., 2013) on  $\mathbf{L}^{\text{new}}$  after each reduction. However, we empirically observed numerical instability and poor convergence when applying the sparsification algorithm. Therefore, we opted for dropping after each reduction the connections with weights below a small threshold  $\epsilon$  (e.g.,  $10^{-4}$ ). We can show that the spectrum of a coarsened Laplacian and, therefore, the spectral interlacing, is preserved up to a small factor that depends on  $\epsilon$ . Let  $\mathbf{Z}$  be the matrix applied to remove small values in a Laplacian  $\mathbf{L}$ , i.e., the weak connections, which is defined as

$$\mathbf{Z} = \begin{cases} Z_{i,j} = -L_{i,j}, & \text{if } |L_{i,j}| \leq \epsilon \\ Z_{i,j} = 0, & \text{otherwise.} \end{cases} \quad (16)$$

**Theorem 1.** *Each eigenvalue  $\bar{\lambda}_i$  of the sparsified Laplacian  $\bar{\mathbf{L}} = \mathbf{L} + \mathbf{Z}$  is bounded by*

$$\bar{\lambda}_i \leq \lambda_i + \frac{\mathbf{v}_i^T \mathbf{Z} \mathbf{v}_i}{\mathbf{v}_i^T \mathbf{v}_i}, \quad (17)$$

where  $\mathbf{v}_i$  is the eigenvector of  $\mathbf{L}$  associated to  $\lambda_i$ .

The proof and an example are in Appendix.

**Pooling with larger stride.** The application of a single decimation matrix  $\mathbf{S}^{(i)}$  corresponds to a classic pooling with stride 2, as it approximately halves the number of nodes. However, pooling with stride  $2^k$  is easily obtained by applying  $k$  decimation matrices in cascade. Fig. 2 shows an example of pooling with approximately stride 8, which allows to skip 2 levels of the graph coarsening and to directly apply a convolution with Laplacian  $\mathbf{L}^{(3)}$  after the first convolution with  $\mathbf{L}^{(0)}$ .

## 5. Experiments

We consider three classification tasks on graph data: node classification, graph signal classification, and graph classification. Since we process only graphs of medium and small sizes, we use Kron reduction (15) in all experiments. However, we advise the reduction in (14) when dealing with very large graphs to avoid memory issues.

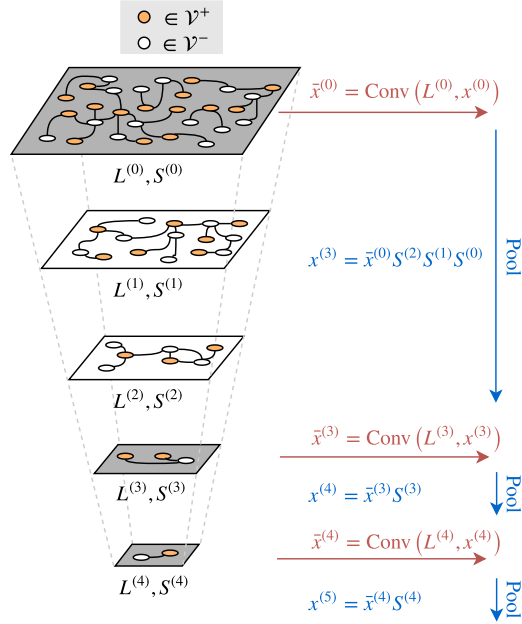


Figure 2. Example of higher-order graph pooling. After the first convolution, the graph is reduced by repeatedly applying the node decimation procedure until the desired graph size is reached.

Table 1. Hyperparameters setting.

Dataset	$L_2$ reg.	$p_{\text{drop}}$	GCN	Cheby	ARMA	W
			$L$	$K$	$[K, T]$ share	
Cora	5e-4	0.75	1	2	[2,1]	–
Citeseer	5e-4	0.75	1	3	[3,1]	–
Pubmed	5e-4	0.0	1	3	[1,4]	no
MNIST	5e-4	0.5	3	25	[5,10]	no
20news	1e-3	0.7	1	5	[1,1]	–
Enzymes	5e-4	0.5	1	3	[1,4]	yes
Proteins	5e-4	0.5	2	10	[3,2]	no
D&D	5e-4	0.0	1	5	[3,4]	yes
MUTAG	5e-4	0.25	3	10	[3,4]	no

In Tab. 1 we report for each dataset the best hyperparameter configurations found with cross-validation. For all filters,  $L_2$  regularization weight and dropout probability ( $p_{\text{drop}}$ ). For GCN, number of stacked graph convolutions ( $L$ ). For Cheby, polynomial order ( $K$ ). For ARMA, number of stacks ( $K$ ), depth ( $T$ ), and usage of shared weights in the GCS layer (share  $\mathbf{W}$ ).

### 5.1. Semi-supervised node classification

The input for this task is a single graph described by an adjacency matrix  $\mathbf{A} \in \mathbb{R}^{M \times M}$ , a graph signal  $\mathbf{X} \in \mathbb{R}^{M \times F_m}$  and the labels  $\mathbf{y}_l \in \mathbb{R}^{M_l}$  of a subset of nodes  $M_l \subset M$ . The target outputs are the labels  $\mathbf{y}_u \in \mathbb{R}^{M_u}$  of the unlabelled nodes. For this task, pooling is not required since the output is computed in the node space by mapping the nodes features to the labels through graph convolutions.

We follow the same experimental setup of Kipf & Welling

Table 2. Node classification accuracy. Best results in bold.

Method	Cora	Citeseer	Pubmed
LP	68.0	45.3	63.0
DW	67.2	43.2	65.3
PL	75.7	64.7	77.2
MoNet	81.7 $\pm 0.5$	—	78.8 $\pm 0.4$
GAT	83.0 $\pm 0.7$	72.5 $\pm 0.7$	79.0 $\pm 0.3$
LNet	80.4 $\pm 1.1$	68.7 $\pm 1.0$	78.3 $\pm 0.3$
Cayley	81.2 $\pm 1.2$	67.1 $\pm 2.4$	75.6 $\pm 3.6$
GCN	81.5 $\pm 0.4$	70.3 $\pm 0.5$	79.0 $\pm 0.3$
Cheby	79.5 $\pm 1.2$	70.1 $\pm 0.8$	74.4 $\pm 1.1$
<b>ARMA</b>	<b>83.5 <math>\pm 0.6</math></b>	<b>73.8 <math>\pm 0.6</math></b>	<b>81.4 <math>\pm 0.3</math></b>

(2016a) on three citation network datasets: Citeseer, Cora and Pubmed. Each dataset is a graph, whose nodes  $\mathbf{x} \in \mathbb{R}^{F_{in}}$  are documents represented by sparse bag-of-words feature vectors. The binary undirected edges in  $\mathbf{A}$  indicate citation links between documents. For training, 20 labels per document class are used ( $\mathbf{y}_l$ ) and the performance is evaluated as classification accuracy on  $\mathbf{y}_u$ .

As in (Kipf & Welling, 2016a), we use a 2-layers GNN with 16 hidden units and we report in Tab. 2 the mean classification accuracy obtained for different filters, namely ChebNets (Defferrard et al., 2016), GCN (Kipf & Welling, 2016a), and the proposed ARMA. We also report results obtained by CayleyNet that, like ARMA, implements rational spectral filters (Levie et al., 2019b). As additional baselines, we include results from the literature obtained by Label Propagation (LP) (Zhou et al., 2004), Deepwalk (DW) (Perozzi et al., 2014), Planetoid (PL) (Yang et al., 2016), Graph Attention Networks (GAT) (Velickovic et al., 2017), LanczosNets (LNet) (Liao et al., 2019), and mixture model networks (MoNet) (Monti et al., 2017).

Node classification is a semi-supervised task that requires a strong regularization and a simple model to avoid overfitting on the few labels available. This is the key of GCN’s success when compared to the more complex filters, such as Chebyshev. However, despite having more powerful modelling capabilities, the proposed ARMA layer has a flexible formulation that allows to obtain the right degree of complexity for each task, leading to a better performance than other approaches. Notably, our method surpasses even GAT, which exploits a sophisticated attention mechanism to dynamically compute the neighbours’ importance during the graph convolution.

## 5.2. Graph signal classification

In this task,  $N$  different graph signals  $\mathbf{X} \in \mathbb{R}^{M \times F_{\text{in}}}$ , defined on the same adjacency matrix  $\mathbf{A} \in \mathbb{R}^{M \times M}$ , must be classified with labels  $\mathbf{y}_1, \dots, \mathbf{y}_N$ . Like in traditional CNNs, this task can be solved by a deep architecture composed of  $L$  graph convolutional layers, each one followed by a pooling layer. In each layer  $l$ , the graph convolu-

Table 3. Graph signal classification (MNIST). The  $p$ -values are computed with respect to the highest mean value in each column.

GC layer	Pooling	
	clust	decim
Cayley	$99.18 \pm 0.1$ ( $p = 0.66$ )	<b><math>99.33 \pm 0.1</math></b>
GCN	$98.48 \pm 0.2$ ( $p < 10^{-4}$ )	$98.46 \pm 0.2$ ( $p < 10^{-4}$ )
Cheby	$99.14 \pm 0.1$ ( $p = 0.19$ )	$99.25 \pm 0.2$ ( $p = 0.27$ )
<b>ARMA</b>	<b><math>99.20 \pm 0.1</math></b>	<b><math>99.33 \pm 0.1</math></b>

tion modifies the vertex features by mapping the graph signal  $\mathbf{x}^{(l)} \in \mathbb{R}^{M_l \times F_l}$  into  $\bar{\mathbf{x}}^{(l)} \in \mathbb{R}^{M_l \times F_{l+1}}$ , while the pooling operation maps  $\bar{\mathbf{x}}^{(l)}$  into a new node space  $\mathbf{x}^{(l+1)} \in \mathbb{R}^{M_{l+1} \times F_{l+1}}$ . In the last layer, the features of the remaining nodes are aggregated by a global operation,  $\mathbf{x} \in \mathbb{R}^{M_L \times F_L} \rightarrow \mathbf{x} \in \mathbb{R}^{F_L}$ , and a Softmax layer computes the labels. We perform experiments following the same setting of Defferrard et al. (2016) for the MNIST and 20news datasets.

**MNIST.** To emulate a classic CNNs operating on a regular 2D grid, an 8-NN graph is defined on the 784 pixel of the MNIST images. The elements in  $\mathbf{A}$  are

$$a_{ij} = \exp\left(-\frac{\|p_i - p_j\|^2}{\sigma^2}\right), \quad (18)$$

where  $p_i$  and  $p_j$  are the 2D coordinates of pixel  $i$  and  $j$ . Each graph signal is a vectorized image  $\mathbf{x} \in \mathbb{R}^{784 \times 1}$ . The network architecture is GC(32)-P(4)-GC(64)-P(4)-FC(512), where GC( $n$ ) indicates a graph convolution with  $n$  filters, P( $s$ ) a pooling operation with stride  $s$ , and FC( $u$ ) a fully connected layer with  $u$  units. As discussed in Sec. 4.1, when using decimation pooling a stride of 4 is obtained by multiplying two decimation matrices in cascade ( $\mathbf{S}^{(1)}\mathbf{S}^{(0)}$  and  $\mathbf{S}^{(3)}\mathbf{S}^{(2)}$  in this case).

Tab. 3 reports the results obtained by using as filter (GC) a stack of GCNs, Cheby, Cayley, or ARMA, and the pooling (P) implemented either with hierarchical clustering (Defferrard et al., 2016) or the proposed node decimation. Results obtained over 10 runs show that ARMA achieves slightly higher mean accuracy, but there is not a statistical significant difference ( $p$ -value  $< 0.05$ ) from the results obtained by Cayley and Cheby filters. The artificial 8-NN graph generated for this task, contrarily to most real-world graphs, is extremely regular and the node pairs are easily matched by the clustering procedure. Nevertheless, pooling implemented with node decimation gains an improvement in accuracy, which is small but significant.

**20news.** The dataset consists of 18,846 documents divided in 20 classes. Each graph signal is a document represented by a bag-of-words of the  $10^4$  most frequent words in the corpus, embedded via Word2vec (Mikolov et al., 2013). The underlying graph of  $10^4$  nodes is defined by a 16-NN adjacency matrix built as in Eq. (18), where  $p_i, p_j$  are the

Table 4. Graph signal classification results on 20news.

Method	Accuracy
Linear SVM	65.90
Multinomial Naive Bayes	68.51
Softmax	66.28
Cayley	$68.84 \pm 0.3$
GCN	$65.45 \pm 0.2$
Cheby	$68.24 \pm 0.2$
<b>ARMA</b>	<b><math>70.02 \pm 0.1</math></b>

embeddings of words  $i$  and  $j$ . We report results obtained with a single convolutional layer (GCN, Cheby, Cayley, or ARMA), followed by softmax. We also include results from the other methods reported in (Defferrard et al., 2016). As in (Defferrard et al., 2016), for Cheby we use 32 filters. Instead, for GCN, Cayley and ARMA, we obtained better results with 16 filters only. The classification accuracy reported in Tab. 4 shows that ARMA significantly outperforms the other models. Since we use only one GCS layer in the ARMA filter ( $K = 1$ ), the main difference between ARMA and GCN in this case is the presence of the skip connection with high dropout, which is shown to have a significant impact on the performance.

### 5.3. Graph classification

In this task, the  $i$ -th datum is a graph represented by a pair  $\{\mathbf{A}_i, \mathbf{X}_i\}$ ,  $i = 1, \dots, N$ , where  $\mathbf{A}_i \in \mathbb{R}^{M_i \times M_i}$  is an adjacency matrix with  $M_i$  nodes, and  $\mathbf{X}_i \in \mathbb{R}^{M_i \times F}$  describes the node features. Each sample must be classified with a label  $y_i$ . To train the GNN on mini-batches of graphs with a variable number of nodes, we compute the disjoint union of the graphs in each mini-batch, and train the network on the obtained Laplacian and graph signal. In this way, it is possible to apply the convolution and pooling operations seamlessly, performing batched computation without resorting to zero-padding. At the end, an average pooling matrix aggregates the features of the remaining nodes for each graph signal, and a softmax layer yields the final output for each graph. Fig. 3 reports an example of the procedure.

To test our model, we consider four datasets from the benchmark database for graph kernels<sup>1</sup>: Enzymes, Proteins, D&D, and MUTAG. We use node degree, clustering coefficients, and node labels as additional node features. For each experiment we adopt a fixed network architecture, GC(64)-P(2)-GC(64)-P(2)-GC(64)-P(2)-AvgPool-Softmax, in order to compare different graph filters and pooling procedures on a common ground. We evaluate model performance in 10-fold cross-validation, using 10% of the training set in each fold as validation set for early stopping. We report in Table 5 the test accuracy averaged

<sup>1</sup><https://ls11-www.cs.tu-dortmund.de/staff/morris/graphkerneldatasets>

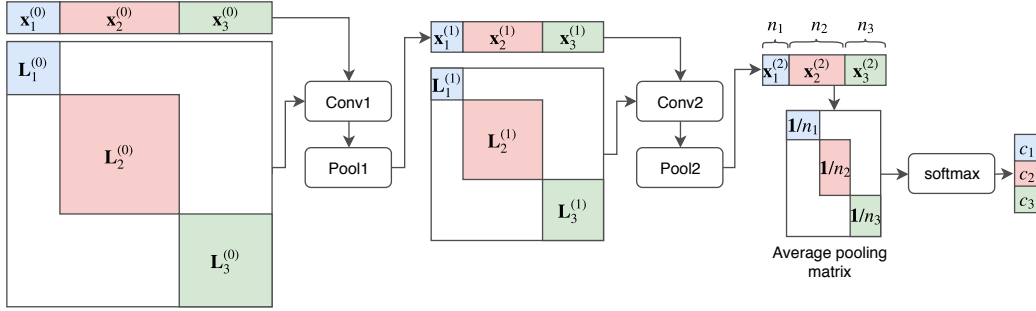


Figure 3. Implementation of graph classification with mini batches.

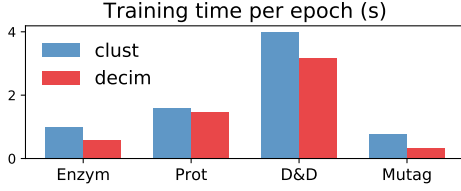


Figure 4. Mean training time per epoch when using ARMA filters and pooling based on hierarchical clustering or decimation.

over the 10 folds. For comparison, Tab. 5 also reports the results obtained by state-of-the-art graph kernels and other neural networks for graph classification: the Weisfeiler-Lehman kernel (WL) (Shervashidze et al., 2011); Edge-Conditioned Convolutional networks (ECCs) (Simonovsky & Komodakis, 2017); PATCHY-SAN (Niepert et al., 2016); GRAPHSAGE (Hamilton et al., 2017); Diffusion-CNNs (DCNNs) (Atwood & Towsley, 2016); GCNs using differential pooling (DIFFPOOL) (Ying et al., 2018); Deep Graph Convolutional Neural Networks (DGCNNs) (Zhang et al., 2018).

The proposed ARMA layer consistently achieves the best performance w.r.t. layers based on polynomial filters showing, once again, the superior modeling capability of the ARMA filter. The combination of ARMA and decimation pooling is particularly effective for the Enzymes dataset, significantly improving over all other tested layers and pooling methods. The same configuration achieves state-of-the-art performance also in MUTAG, and competitive results in Protein. Finally, results on D&D are below the state of the art, suggesting that the adopted architecture is not optimal for this task.

Contrarily to the results obtained on the artificial grid on MNIST, here the decimation pooling strategy shows notable improvements over hierarchical clustering, proving to be a more effective technique on irregular graph structures with a variable number of nodes. Moreover, Fig. 4 shows how the overall training time is lower when using decimation pooling w.r.t. hierarchical clustering. Indeed, in cluster pooling, fake nodes must be added whenever the number of nodes is not divisible by  $2^L$  (in our case  $L = 3$ , since we apply pooling 3 times), which implies larger graphs and slower convolutions.

Table 5. Graph classification results.

	Method	Enzymes	Protein	D&D	MUTAG
	WL	53.53	72.92	74.02	80.72
	ECC	53.50	72.65	74.10	89.44
	PATCHY-SAN	–	75.00	76.27	92.63
	GRAPHSAGE	54.25	70.48	75.42	–
	DCNN	18.10	61.29	58.09	66.98
	DIFFPOOL	62.53	<b>76.25</b>	<b>80.64</b>	–
	DGCNN	–	75.54	79.73	85.83
clust	GCN	64.83	72.06	64.60	76.13
	Cheby	66.50	69.19	66.81	80.32
	<b>ARMA</b>	67.83	71.92	71.22	85.67
decim	GCN	67.33	72.15	70.63	86.20
	Cheby	66.50	70.79	68.09	90.39
	<b>ARMA</b>	<b>69.66</b>	75.12	74.86	<b>93.25</b>

## 6. Conclusions

We proposed a graph convolutional layer based on ARMA graph filters, implemented as a recurrent operator. Our formulation allows for a distributed implementation, and is based of efficient sparse tensor operations between the graph Laplacian and node features. For deeper architectures, we adopted a pooling strategy based on node decimation, which achieves superior performance on real-world graphs with irregular topology and faster training times w.r.t. pooling based on graph clustering.

The proposed ARMA layer outperforms existing convolutional layers based on polynomial filters on all classification tasks on graph data taken into account, often outperforming the previous state of the art on several tasks.

The current formulation of the ARMA layer only considers node information, but can be extended to incorporate edge features to weight the contribution of each neighbour differently, as in the edge-conditioned convolutions (Simonovsky & Komodakis, 2017). The results presented in (Velickovic et al., 2017) show a notable increase in performance when applying multi-head soft attention to the Laplacian in a GNN. Given that the ARMA layer is already structured in a parallel fashion, a similar extension based on the attention mechanism could provide comparable benefits, and further improve the performance.



## References

- Atwood, James and Towsley, Don. Diffusion-convolutional neural networks. In *Advances in Neural Information Processing Systems*, pp. 1993–2001, 2016.
- Bacciu, Davide, Errica, Federico, and Micheli, Alessio. Contextual graph markov model: A deep and generative approach to graph processing. In *Proceedings of the 35th international conference on Machine learning*. ACM, 2018.
- Batson, Joshua, Spielman, Daniel A, Srivastava, Nikhil, and Teng, Shang-Hua. Spectral sparsification of graphs: theory and algorithms. *Communications of the ACM*, 56(8):87–94, 2013.
- Battaglia, Peter W, Hamrick, Jessica B, Bapst, Victor, Sanchez-Gonzalez, Alvaro, Zambaldi, Vinicius, Malinowski, Mateusz, Tacchetti, Andrea, Raposo, David, Santoro, Adam, Faulkner, Ryan, et al. Relational inductive biases, deep learning, and graph networks. *arXiv preprint arXiv:1806.01261*, 2018.
- Bruna, Joan, Zaremba, Wojciech, Szlam, Arthur, and LeCun, Yann. Spectral networks and locally connected networks on graphs. *arXiv preprint arXiv:1312.6203*, 2013.
- Defferrard, Michaël, Bresson, Xavier, and Vandergheynst, Pierre. Convolutional neural networks on graphs with fast localized spectral filtering. In *Advances in Neural Information Processing Systems*, pp. 3844–3852, 2016.
- Duvenaud, David K, Maclaurin, Dougal, Iparraguirre, Jorge, Bombarell, Rafael, Hirzel, Timothy, Aspuru-Guzik, Alán, and Adams, Ryan P. Convolutional networks on graphs for learning molecular fingerprints. In *Advances in neural information processing systems*, pp. 2224–2232, 2015.
- Fey, Matthias, Lenssen, Jan Eric, Weichert, Frank, and Müller, Heinrich. Splinecnn: Fast geometric deep learning with continuous b-spline kernels. In *Proceedings of the IEEE Conference on Computer Vision and Pattern Recognition*, pp. 869–877, 2018.
- Gallicchio, Claudio and Micheli, Alessio. Graph echo state networks. In *Neural Networks (IJCNN), The 2010 International Joint Conference on*, pp. 1–8. IEEE, 2010.
- Grattarola, Daniele, Zambon, Daniele, Alippi, Cesare, and Livi, Lorenzo. Change detection in graph streams by learning graph embeddings on constant-curvature manifolds. *arXiv preprint arXiv:1805.06299*, 2018.
- Hamilton, Will, Ying, Zhitao, and Leskovec, Jure. Inductive representation learning on large graphs. In *Advances in Neural Information Processing Systems*, pp. 1024–1034, 2017.
- Henaff, Mikael, Bruna, Joan, and LeCun, Yann. Deep convolutional networks on graph-structured data. *arXiv preprint arXiv:1506.05163*, 2015.
- Holme, Petter. Modern temporal network theory: a colloquium. *The European Physical Journal B*, 88(9):234, 2015.
- Isufi, Elvin, Loukas, Andreas, Simonetto, Andrea, and Leus, Geert. Autoregressive moving average graph filtering. *arXiv preprint arXiv:1602.04436*, 2016.
- Kipf, Thomas N and Welling, Max. Semi-supervised classification with graph convolutional networks. In *International Conference on Learning Representations (ICLR)*, 2016a.
- Kipf, Thomas N and Welling, Max. Variational graph auto-encoders. In *NIPS Workshop on Bayesian Deep Learning*, 2016b.
- Krizhevsky, Alex, Sutskever, Ilya, and Hinton, Geoffrey E. Imagenet classification with deep convolutional neural networks. In *Advances in neural information processing systems*, pp. 1097–1105, 2012.
- Levie, Ron, Elvin, Isufi, and Gitta, Kutyniok. On the transferability of spectral graph filters. *arXiv preprint*, 2019a.
- Levie, Ron, Monti, Federico, Bresson, Xavier, and Bronstein, Michael M. Cayleynets: Graph convolutional neural networks with complex rational spectral filters. *IEEE Transactions on Signal Processing*, 67(1):97–109, Jan 2019b. ISSN 1053-587X. doi: 10.1109/TSP.2018.2879624.
- Li, Qimai, Han, Zhichao, and Wu, Xiao-Ming. Deeper insights into graph convolutional networks for semi-supervised learning. In *Proceedings of AAAI Conference on Artificial Intelligence*, 2018.
- Liao, Renjie, Zhao, Zhizhen, Urtasun, Raquel, and Zemel, Richard. Lanczosnet: Multi-scale deep graph convolutional networks. In *International Conference on Learning Representations (ICLR)*, 2019.
- Loukas, Andreas, Simonetto, Andrea, and Leus, Geert. Distributed autoregressive moving average graph filters. *IEEE Signal Processing Letters*, 22(11):1931–1935, 2015.
- Micheli, Alessio. Neural network for graphs: A contextual constructive approach. *IEEE Transactions on Neural Networks*, 20(3):498–511, 2009.
- Mikolov, Tomas, Chen, Kai, Corrado, Greg, and Dean, Jeffrey. Efficient estimation of word representations in vector space. In *ICLR (Workshop)*, 2013.

- Monti, Federico, Boscaini, Davide, Masci, Jonathan, Rodola, Emanuele, Svoboda, Jan, and Bronstein, Michael M. Geometric deep learning on graphs and manifolds using mixture model cnns. In *Proceedings of the IEEE Conference on Computer Vision and Pattern Recognition*, volume 1, pp. 3, 2017.
- Narang, Sunil K and Ortega, Antonio. Local two-channel critically sampled filter-banks on graphs. In *Image Processing (ICIP), 2010 17th IEEE International Conference on*, pp. 333–336. IEEE, 2010.
- Narang, Sunil K, Gadde, Akshay, and Ortega, Antonio. Signal processing techniques for interpolation in graph structured data. In *Acoustics, Speech and Signal Processing (ICASSP), 2013 IEEE International Conference on*, pp. 5445–5449. IEEE, 2013.
- Niepert, Mathias, Ahmed, Mohamed, and Kutzkov, Konstantin. Learning convolutional neural networks for graphs. In *International conference on machine learning*, pp. 2014–2023, 2016.
- Page, Lawrence, Brin, Sergey, Motwani, Rajeev, and Winograd, Terry. The pagerank citation ranking: Bringing order to the web. Technical report, Stanford InfoLab, 1999.
- Perozzi, Bryan, Al-Rfou, Rami, and Skiena, Steven. Deepwalk: Online learning of social representations. In *Proceedings of the 20th ACM SIGKDD international conference on Knowledge discovery and data mining*, pp. 701–710. ACM, 2014.
- Scarselli, Franco, Gori, Marco, Tsoi, Ah Chung, Hagenbuchner, Markus, and Monfardini, Gabriele. The graph neural network model. *IEEE Transactions on Neural Networks*, 20(1):61–80, 2009.
- Shervashidze, Nino, Schweitzer, Pascal, Leeuwen, Erik Jan van, Mehlhorn, Kurt, and Borgwardt, Karsten M. Weisfeiler-lehman graph kernels. *Journal of Machine Learning Research*, 12(Sep):2539–2561, 2011.
- Shuman, David I, Vandergheynst, Pierre, and Frossard, Pascal. Chebyshev polynomial approximation for distributed signal processing. In *Distributed Computing in Sensor Systems and Workshops (DCOSS), 2011 International Conference on*, pp. 1–8. IEEE, 2011.
- Shuman, David I, Faraji, Mohammad Javad, and Vandergheynst, Pierre. A multiscale pyramid transform for graph signals. *IEEE Transactions on Signal Processing*, 64(8):2119–2134, 2016.
- Simonovsky, Martin and Komodakis, Nikos. Dynamic edge-conditioned filters in convolutional neural networks on graphs. In *Proceedings of the IEEE Conference on Computer Vision and Pattern Recognition*, 2017.
- Susnjara, Ana, Perraudin, Nathanael, Kressner, Daniel, and Vandergheynst, Pierre. Accelerated filtering on graphs using lanczos method. *arXiv preprint arXiv:1509.04537*, 2015.
- Tremblay, Nicolas, Goncalves, Paulo, and Borgnat, Pierre. Design of graph filters and filterbanks. In *Cooperative and Graph Signal Processing*, pp. 299–324. Elsevier, 2018.
- Velickovic, Petar, Cucurull, Guillem, Casanova, Arantxa, Romero, Adriana, Lio, Pietro, and Bengio, Yoshua. Graph attention networks. *arXiv preprint arXiv:1710.10903*, 2017.
- Wu, Yonghui, Schuster, Mike, Chen, Zhifeng, Le, Quoc V, Norouzi, Mohammad, Macherey, Wolfgang, Krikun, Maxim, Cao, Yuan, Gao, Qin, Macherey, Klaus, et al. Google’s neural machine translation system: Bridging the gap between human and machine translation. *arXiv preprint arXiv:1609.08144*, 2016.
- Yang, Zhilin, Cohen, William W, and Salakhutdinov, Ruslan. Revisiting semi-supervised learning with graph embeddings. In *Proceedings of the 33rd International Conference on International Conference on Machine Learning-Volume 48*, pp. 40–48. JMLR. org, 2016.
- Ying, Rex, You, Jiaxuan, Morris, Christopher, Ren, Xiang, Hamilton, William L, and Leskovec, Jure. Hierarchical graph representation learning with differentiable pooling. *arXiv preprint arXiv:1806.08804*, 2018.
- Zhang, Muhan, Cui, Zhicheng, Neumann, Marion, and Chen, Yixin. An end-to-end deep learning architecture for graph classification. In *Proceedings of AAAI Conference on Artificial Intelligence*, 2018.
- Zhou, Denny, Bousquet, Olivier, Lal, Thomas N, Weston, Jason, and Schölkopf, Bernhard. Learning with local and global consistency. In *Advances in neural information processing systems*, pp. 321–328, 2004.

## Appendix

### A. Spectral analysis of Kron reduction with sparification

Kron reduction guarantees spectral interlacing between the original Laplacian  $\mathbf{L} \in \mathbb{R}^{N \times N}$  and the new coarsened one  $\bar{\mathbf{L}} \in \mathbb{R}^{M \times M}$ , with  $M < N$ , i.e., given the spectrum  $\bar{\Lambda}$  of  $\bar{\mathbf{L}}$  and the spectrum  $\Lambda$  of  $\mathbf{L}$ , we have  $\lambda_i \geq \bar{\lambda}_i \geq \lambda_{N-M+i}$ ,  $\forall i = 1, \dots, M$ ,  $\lambda_i \in \Lambda$ , and  $\bar{\lambda}_i \in \bar{\Lambda}$ . By repeatedly applying Kron reduction the coarsened graph becomes more and more dense and the connectivity less localized, introducing computational drawbacks. To limit the growth of non-zero entries after each reduction, we sparsify the reduced matrix by dropping connections with weights below a small threshold  $\epsilon$ . It is possible to show that after this operation the spectrum of the coarsened Laplacian is preserved, up to a small factor that depends on  $\epsilon$ .

Let  $\mathbf{Z}$  be the matrix applied to remove small values in the Laplacian  $\mathbf{L}$ , i.e., the weak connections, which is defined as

$$\mathbf{Z} = \begin{cases} Z_{i,j} = -L_{i,j}, & \text{if } |L_{i,j}| \leq \epsilon \\ Z_{i,j} = 0, & \text{otherwise.} \end{cases}$$

**Theorem 2.** Each eigenvalue  $\bar{\lambda}_i$  of the sparified Laplacian  $\bar{\mathbf{L}} = \mathbf{L} + \mathbf{Z}$  is bounded by

$$\bar{\lambda}_i \leq \lambda_i + \frac{\mathbf{v}_i^T \mathbf{Z} \mathbf{v}_i}{\mathbf{v}_i^T \mathbf{v}_i},$$

where  $\mathbf{v}_i$  is the eigenvector of  $\mathbf{L}$  associated to  $\lambda_i$ .

*Proof.* Let  $\mathbf{P}$  be a matrix with elements  $P_{i,j} = \text{sign}(Z_{i,j})$  and consider the perturbation  $\mathbf{L} + \epsilon \mathbf{P}$ , which modifies the eigenvalue problem  $\mathbf{L} \mathbf{v}_i = \lambda_i \mathbf{v}_i$  in

$$(\mathbf{L} + \epsilon \mathbf{P})(\mathbf{v}_i + \mathbf{v}_\epsilon) = (\lambda_i + \lambda_\epsilon)(\mathbf{v}_i + \mathbf{v}_\epsilon). \quad (19)$$

where  $\lambda_\epsilon$  and  $\mathbf{v}_\epsilon$  are small perturbations on the eigenvalues and eigenvectors, respectively, to be estimated. By expanding (19), then canceling the equation  $\mathbf{L} \mathbf{v}_i = \lambda_i \mathbf{v}_i$  and the high order terms  $\mathcal{O}(\epsilon^2)$ , one obtains

$$\mathbf{L} \mathbf{v}_\epsilon + \epsilon \mathbf{P} \mathbf{v}_i = \lambda_i \mathbf{v}_\epsilon + \lambda_\epsilon \mathbf{v}_i \quad (20)$$

Since  $\mathbf{L}$  is symmetric, its eigenvectors can be used as a basis to express the perturbed eigenvectors

$$\mathbf{v}_\epsilon = \sum_{j=1}^N \delta_{ij} \mathbf{v}_j \quad (21)$$

where  $\delta_{ij}$  are (small) unknown coefficients. Substituting (21) in (20) and bringing  $\mathbf{L}$  inside the sum, gives

$$\sum_{j=1}^N \delta_{ij} \mathbf{L} \mathbf{v}_j + \epsilon \mathbf{P} \mathbf{v}_i = \lambda_i \sum_{j=1}^N \delta_{ij} \mathbf{v}_j + \lambda_\epsilon \mathbf{v}_i \quad (22)$$

By applying the original eigenvalue problem that gives  $\sum_{j=1}^N \delta_{ij} \mathbf{L} \mathbf{v}_j = \sum_{j=1}^N \delta_{ij} \lambda_j \mathbf{v}_j$  and by left-multiplying each term with  $\mathbf{v}_i^T$ , (22) becomes

$$\mathbf{v}_i^T \sum_{j=1}^N \delta_{ij} \lambda_j \mathbf{v}_j + \mathbf{v}_i^T \epsilon \mathbf{P} \mathbf{v}_i = \mathbf{v}_i^T \lambda_i \sum_{j=1}^N \delta_{ij} \mathbf{v}_j + \mathbf{v}_i^T \lambda_\epsilon \mathbf{v}_i \quad (23)$$

Since the eigenvectors are orthogonal,  $\mathbf{v}_i^T \mathbf{v}_j = 0, \forall j \neq i$ . Then, (23) becomes

$$\mathbf{v}_i^T \delta_{ii} \lambda_i \mathbf{v}_i + \mathbf{v}_i^T \epsilon \mathbf{P} \mathbf{v}_i = \mathbf{v}_i^T \lambda_i \delta_{ii} \mathbf{v}_i + \mathbf{v}_i^T \lambda_i \mathbf{v}_i \rightarrow \mathbf{v}_i^T \epsilon \mathbf{P} \mathbf{v}_i = \mathbf{v}_i^T \lambda_\epsilon \mathbf{v}_i$$

which gives

$$\lambda_\epsilon = \frac{\mathbf{v}_i^T \epsilon \mathbf{P} \mathbf{v}_i}{\mathbf{v}_i^T \mathbf{v}_i} \geq \frac{\mathbf{v}_i^T \mathbf{Z} \mathbf{v}_i}{\mathbf{v}_i^T \mathbf{v}_i}, \quad \text{since } \mathbf{Z} \leq \epsilon \mathbf{P}$$

□

### A.1. Example

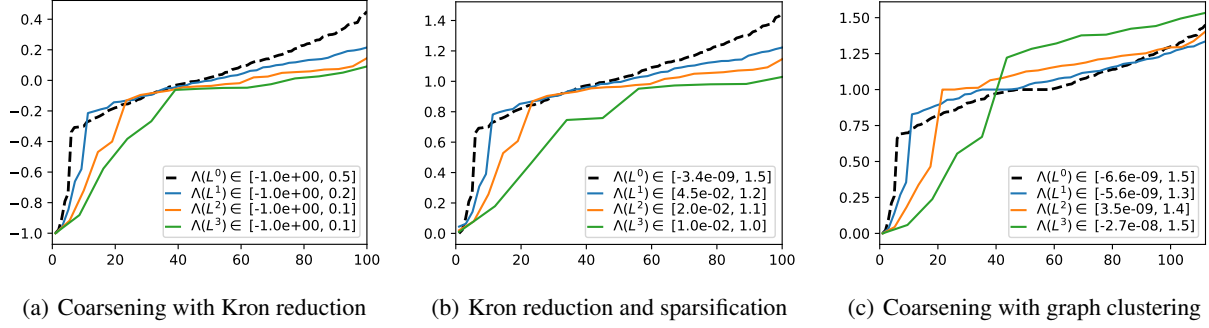


Figure 5. Spectrum of the original Laplacian,  $\Lambda(\mathbf{L}^0)$ , and of the reduced Laplacians after  $n$  applications of graph coarsening  $\Lambda(\mathbf{L}^n)$ . Fig (a) shows that Kron reduction preserves spectral interlacing. Fig (b) shows that the proposed sparsification preserves very well the original spectra. On the other hand, Fig (c) shows that by reducing the graph by means of node clustering there is no more spectral interlacing between the original Laplacian and the coarsened ones.

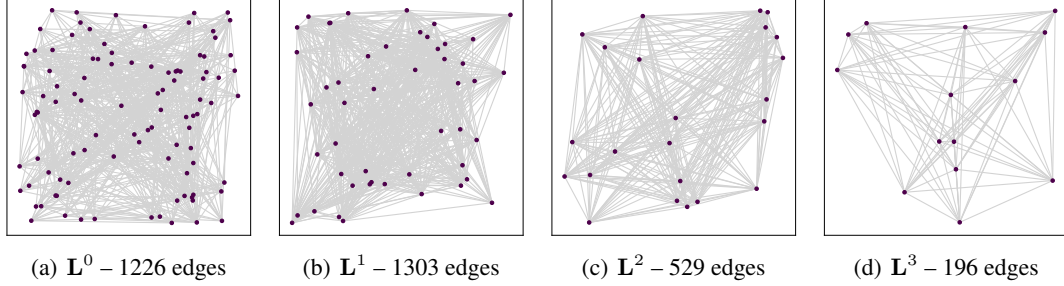


Figure 6. Laplacians coarsened with Kron reduction.

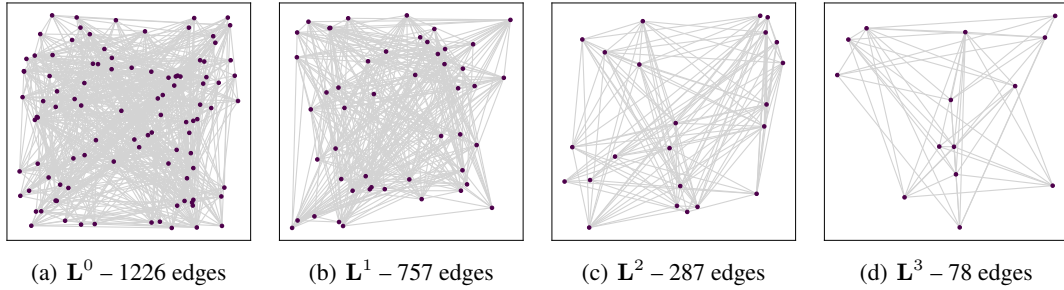


Figure 7. Laplacians coarsened with Kron reduction after applying the proposed sparsification method.

Fig. 5 shows that the original spectrum  $\Lambda(\mathbf{L}^0)$  in practice is preserved in the coarsened Laplacians  $\mathbf{L}^1$ ,  $\mathbf{L}^2$ , and  $\mathbf{L}^3$ , after applying Kron reduction with the proposed sparsification operation with a small  $\epsilon$  (in the example and in all our experiments,  $\epsilon = 1E - 4$ ). On the other hand, when using graph clustering (e.g., GRACCLUS) to coarsen the Laplacians, those do not preserve spectral interlacing.

Fig. 6 shows the edges in the original Laplacian,  $\mathbf{L}^0$ , and those obtained after Kron reduction. Fig. 7 instead, shows the edges that remain after applying the proposed sparsification method.